201969: gold grains, Coolyia Creek prospect

(Hardey Formation, Marble Bar Sub-basin)

Sample type	Gold grains
Specimens	Four specimens comprising four grains
Total weight	2.2 g (1.2 g, 0.4 g, 0.3 g, 0.3 g)
Sample location	Coolyia Creek prospect, about 34 km southwest of Marble Bar
Coordinates	MGA zone 50, 763670E 7630530N
Datum	GDA94
1:250 000 map sheet	MARBLE BAR (SF 50-8)
1:100 000 map sheet	MARBLE BAR (2855)
Tenement	E 45/4965
Collector	Castle Minerals Limited

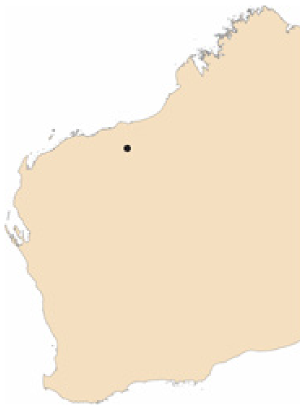

Location and sampling

The sample was provided by Castle Minerals Limited in October 2018. It was collected at the Coolyia Creek prospect in the east Pilbara region. The sample comprises four gold grains recovered from colluvium (Castle Minerals Limited, 2018, written comm., 23 October).

Geological context

The gold grains at the Coolyia Creek prospect were collected from colluvium that overlies a cobble to boulder conglomerate unit in the 2766–2749 Ma Hardey Formation (Hickman, 2020), close to Archean quartz reefs (Castle Minerals Limited, 2018, written comm., 23 October). The prospect is located in the Marble Bar Sub-basin of the Fortescue Basin (Hickman, 2021a), about 3.4 km southwest of the significant, basin-bounding Split Rock Shear Zone (GSWA, 2014; Hickman and Van Kranendonk, 2008).

The Hardey Formation conglomerate unit comprises well-rounded clasts of Mount Roe Basalt and granitic rocks in a matrix of quartzofeldspathic sandstone that includes mafic volcanic detritus (Hickman, 2020; GSWA, 2014). The panel of Fortescue Group rocks overlies Pilbara basement rocks (Warrawoona Group; Hickman, 2021c) and nearby is surrounded by outcrops of the overlying 2750–2727 Ma Kylena Formation (Hickman, 2021b; GSWA, 2014).

The nearest mapped regolith landform is an alluvial–fluvial unit comprising unconsolidated sand, silt, and gravel in active, but poorly defined, drainage channels on a floodplain (GSWA, 2014).

Methodology

The gold specimens were photographed and weighed, their overall morphology and external features, such as colour, roundness, surface relief, coatings, mineral inclusions and mineralogical assemblages, were recorded using visual morphometry. The raw surfaces of the samples were analysed using scanning electron microscopy with energy dispersive X-ray spectroscopy (SEM-EDS). The specimens were mounted in epoxy resin and polished to expose their microstructure and inclusions for examination using reflected-light microscopy and SEM-EDS. Gold microchemistry was determined by laser ablation inductively coupled plasma mass spectrometry (LA-ICP-MS), calibrated against certified gold reference materials (CRM; Murray, 2009). The samples were ablated in duplicate or triplicate along 0.5 mm-long traverses and average values calculated for elements present in the CRM. Gold surfaces were repolished after laser ablation, etched with aqua regia, and internal structures examined using reflected-light microscopy. Details of this method are described in Hancock and Beardsmore (2020).

Morphology

The sample comprises four gold specimens: A, B, C and D (Fig. 1).

Specimen A is a gold–quartz intergrowth with dimensions 10 × 8 × 4 mm. It is moderately rounded over parts of its surface and is light brown where it is thinly coated with Fe-oxide minerals and clays (Fig. 1a).

Specimen B is a well-rounded intergrowth of gold, quartz and Fe-oxide minerals, with dimensions 7 × 5 × 3 mm. Its surface is compacted, and is almost entirely dark brown (Fig. 1b).

Specimen C is an elongate (broadly prolate) and moderately rounded gold grain, with dimensions 8 × 3 × 2 mm. It has a patchy coating of Fe-rich clays (Fig. 1c).

Specimen D is a highly irregular and flattened gold grain, with dimensions 7 × 6 × 2 mm. Its surface is moderately rounded, and has no visible coatings or inclusions (Fig. 1d).

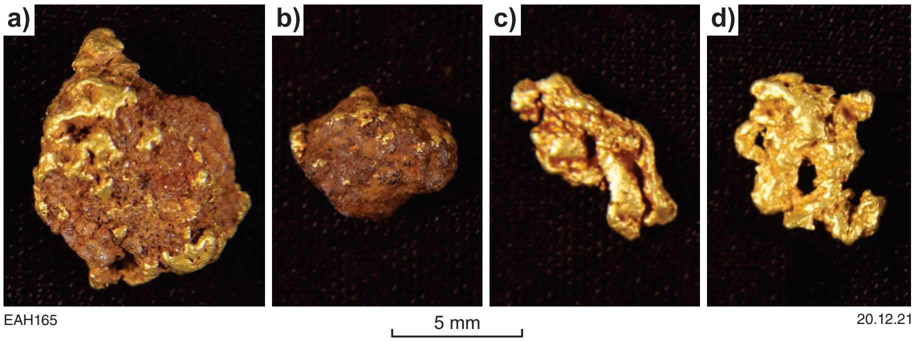

Figure 1. **Four gold grains comprise sample 201969: gold grains, Coolyia Creek prospect: a) specimen A; b) specimen B; c) specimen C; d) specimen D**

SEM-EDS analysis of raw surfaces

The surface of specimen A comprises gold with 2–7% Ag, and subordinate quartz. Pits in the surface are lined with mixed illite and low-Fe, Mg-rich clays (Fig. 2a). Very fine, spongy gold particles are commonly agglomerated along the boundaries between gold and quartz (Fig. 2b).

The surface of specimen B appears more damaged and compacted than in specimen A, and comprises a mixture of gold and minor quartz, goethite and Fe-rich clays (Fig. 2c).

The surfaces of specimens C and D are smooth and pitted (Fig. 2d), and consist mainly of gold with no detectable Ag.

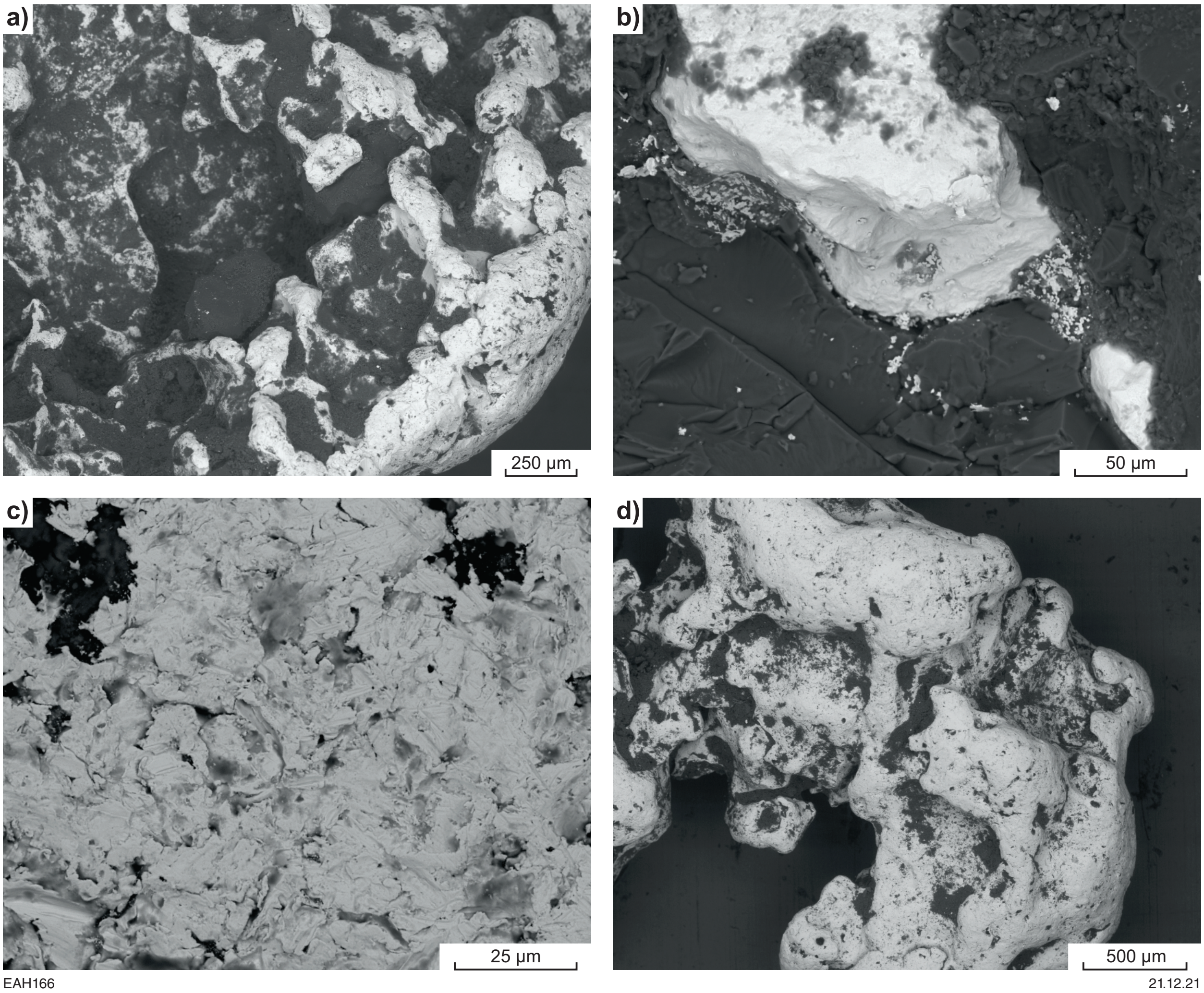

Figure 2. **Backscattered electron images (BSE) of sample 201969: gold grains, Coolyia Creek prospect: a) specimen A; b) specimen B; c) specimen C; d) specimen D**

Optical microscopy of polished surfaces

The gold in specimen A fills spaces between quartz grains, with smooth but irregular contacts. Quartz is intensively granulated and partially disintegrated (Fig. 3a).

Gold in specimen B occurs in ragged masses and is finely disseminated in a mixture of spongy goethite and isolated grains of quartz. The massive gold contains small (50–80 μm), subhedral inclusions of sulfide minerals (Fig. 3b).

Massive gold in specimen C contains irregular grains of ilmenite with very fine-grained gold inclusions. Fine gold is also disseminated in clay–quartz mixtures filling the external voids (Fig. 3c).

Specimen D consists of massive irregular gold with minimal quartz and very small ilmenite and pyrite inclusions. Short external intergranular veinlets in gold are filled with clays, quartz, goethite, and small fine-grained gold particles (Fig. 3d).

SEM-EDS analysis of polished surfaces

Massive gold contains Ag from 1.5% in intergranular veinlets to 6% in specimen D. There is no detectable Ag in the very fine-grained, disseminated gold particles.

Massive gold in specimen A contains no inclusions other than quartz.

A subhedral sulfide inclusion in massive gold in specimen B (Fig. 4a) is cobaltite (48% arsenic, 28% cobalt, 16% sulphur, 4% iron, and 4% nickel). Inclusions in specimens C and D comprise ilmenite, pyrite and unidentified Al-oxide minerals. Some of the fine, disseminated, Ag-free gold in specimen C occurs between ilmenite grains, possibly in association with fine-grained rutile (Fig. 4b).

LA-ICP-MS analysis

Analyses consistently detected Ag, Cu and Hg within the gold grains, in concentrations higher than the instrumental detection limit, and probably occurring as limited solid solutions in the gold. Other trace elements were detected only sporadically in low (sub-ppm) concentrations, possibly occurring in micro- and nano-inclusions.

The gold specimens all contain low Ag (3.6 – 4.5%) and Cu (143–279 ppm) and relatively high Hg (970–1046 ppm), although specimen C has higher than average Cu (579 ppm), and specimen D contains up to 6.2% Ag and lower Hg (412–856 ppm), and a wider variety of other trace elements. Small concentrations of Mg are consistently present in each nugget (Table 1). Traces (ppb-level) of Ti, Cr, Ni, Zn, Se, Pd, Sn, Sb, Pb and Bi are present in all four gold grains (Table 2).

Acid etching

The internal fabrics of massive gold in all nuggets are polycrystalline, and exhibit variable degrees of deformation (Fig. 5).

In specimen A the polycrystalline texture is partly recrystallized, with variably coherent twinning and sporadic narrow gold veinlets along curved grains boundaries (Fig. 5a).

Gold in specimen B is mostly finely crystalline with small islands of more coarsely crystalline gold towards the centres of gold masses, indicating near-complete recrystallization by mechanical and chemical supergene processes, such as corrosion. Cobaltite inclusions occur in the more finely crystalline marginal domains in the gold (Fig. 5b).

Gold in specimen C is mostly relatively coarsely polycrystalline, although crystal structures are deformed, showing broken and curved crystal boundaries, lattice translation lines and subgrains. There are thin (50 μm) rims of very fine-grained gold crystals (Fig. 5c).

Gold in specimen D is only mildly deformed. The predominant, relatively coarse-grained crystals show some curviplanar boundaries and twin planes. There is a discontinuous thin (20 μm) outer rim of finely recrystallized gold (Fig. 5d).

Interpretation

All four nuggets are probably derived from a single primary bedrock source, although they have subsequently undergone different transportation and alteration histories. Specimens A and D are the least affected. Specimen C shows some mechanical deformation. Specimen B is the most deformed and chemically altered, although the central domain of constituent gold masses preserves original textural and chemical signatures.

The gold specimens contain pyrite, ilmenite, cobaltite and other unidentified Co–As–Ti inclusions. These mineral inclusions differ to those in a sample of brecciated, gold-bearing vein quartz collected from the same general region (sample 201997, GSWA, preliminary data), in which gold is intergrown with variably oxidized Bi–Pb telluride minerals, and the associated quartz contains inclusions of galena. This suggests that these two samples were formed by separate geological processes.

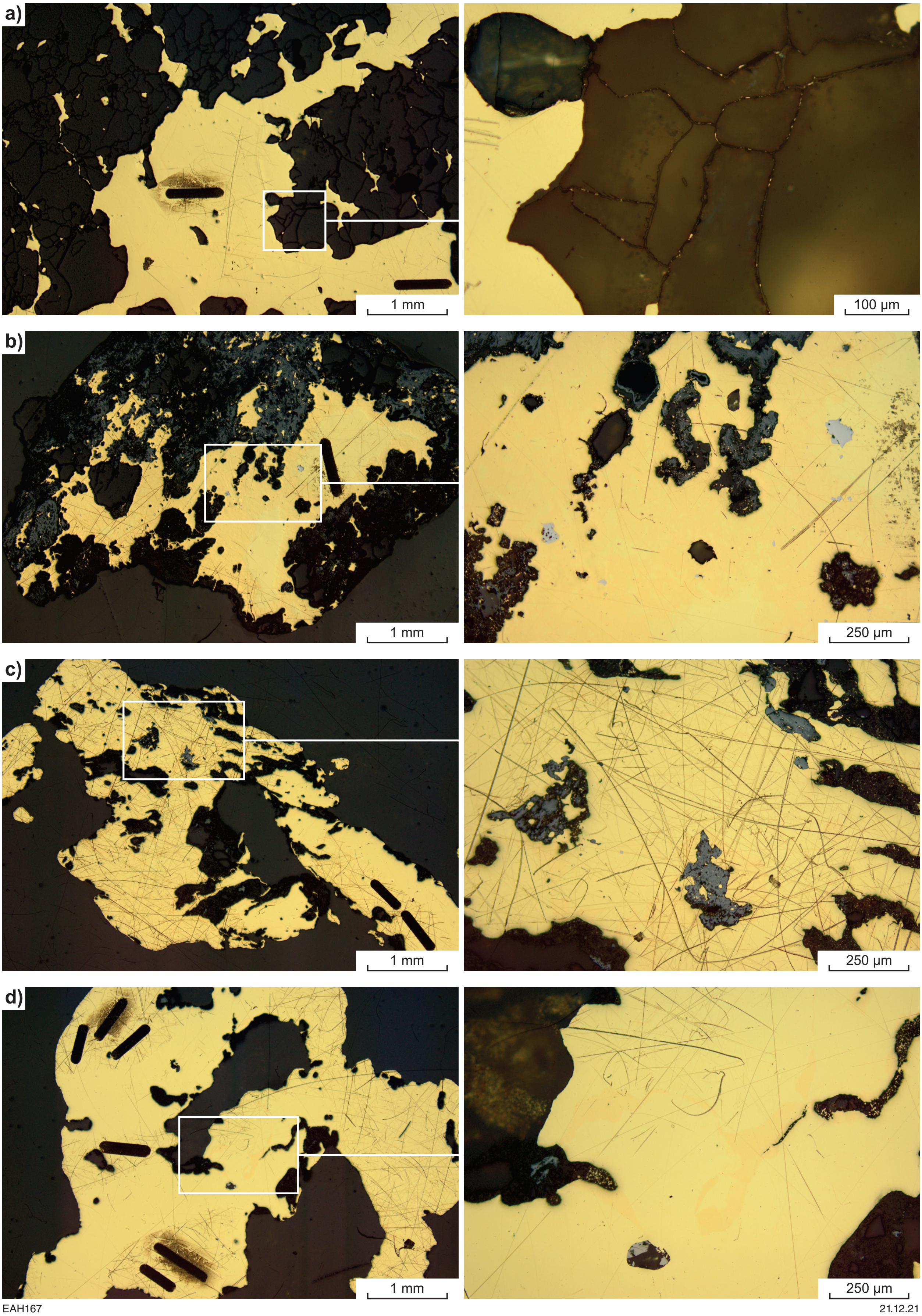

Figure 3. Reflected-light photomicrographs of polished surface of sample 201969: gold grains, Coolyia Creek prospect: a) specimen A; b) specimen B; c) specimen C; d) specimen D. Dark elongate lines are laser ablation tracks produced during LA-ICP-MS analyses

Table 1. LA-ICP-MS data for selected elements in sample 201969: gold grains, Coolyia Creek prospect

Specimen	*Ag (%)*	*Cu (ppm)*	*Hg (ppm)*	*Minor elements (ppm)*
A	3.9, 4.0	164, 226	986, 1046	Mg (1)
B	4.3	143	970	Mg (4)
C	4.8	519	1014	Mg (2), Cr (1)
D	3.6, 4.5, 6.0, 6.2	197, 202, 241, 260	412, 445, 680, 856	Mg (2-5), As (2), Zn (2), Se (1), Cr (1)

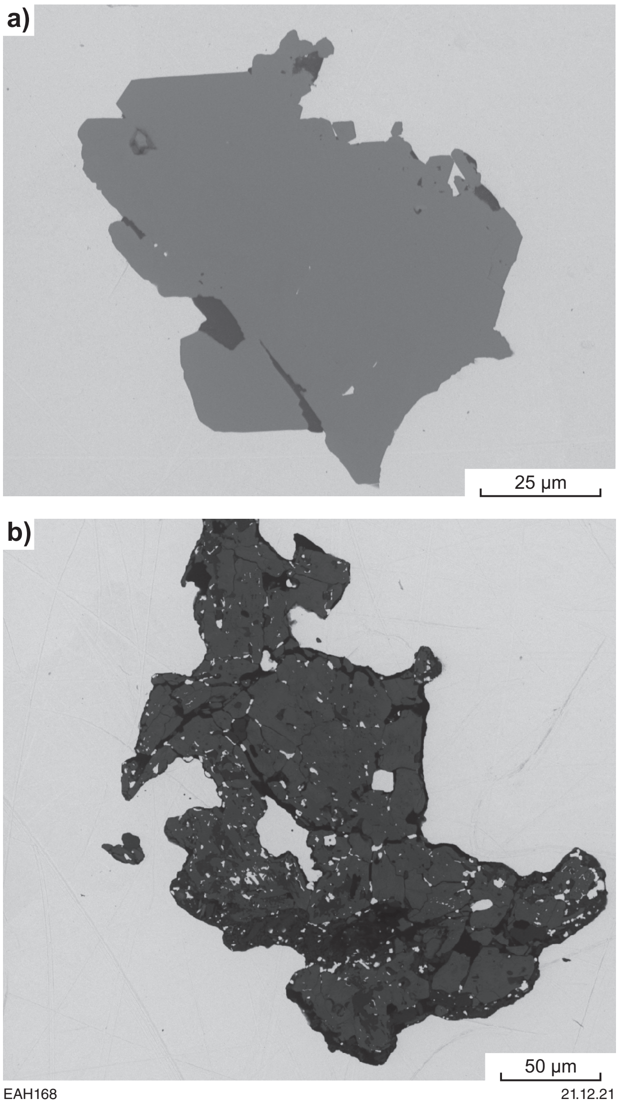

Figure 4. BSE images of mineral inclusions in polished surface of sample 201969: gold grains, Coolyia Creek prospect: a) specimen B; b) specimen C

Table 2. LA-ICP-MS compositional data for sample 201969: gold grains, Coolyia Creek prospect

Specimen and laser ablation line	*Unit*	^{7}*Li*	^{9}*Be*	^{11}*B*	^{23}*Na*	^{25}*Mg*	^{27}*Al*	^{29}*Si*	^{44}*Ca*	^{45}*Sc*	^{49}*Ti*	^{51}*V*	^{53}*Cr*	^{55}*Mn*	^{57}*Fe*	^{59}*Co*	^{60}*Ni*	^{65}*Cu*
A-1	cps		1			75	126				6		3			2		27922
A-2	cps					92	1105				9	2	14			2	5	20323
B	cps					347	277				5		4			7		17745
C	cps			43		185	238				2	1	88			4	11	36205
D-1	cps		2			22	29				7		6		3	3	4	29813
D-2	cps		3			31	89				3					2	5	25027
D-3	cps					457	466				6		99			4	8	13730
D-4	cps					194	364		8		11		95					18094
A-1	ppm					0.90					0.12							226
A-2	ppm					1.10					0.19						0.05	164
B	ppm					4.16					0.10							143
C	ppm					1.80					0.05		1.35				0.17	519
D-1	ppm					0.26					0.14						0.04	240.82
D-2	ppm					0.37					0.07						0.05	202.16
D-3	ppm					4.45					0.11		1.52				0.13	197
D-4	ppm					1.90			0.13		0.19		1.46					260

Specimen and laser ablation line	*Unit*	^{66}*Zn*	^{69}*Ga*	^{72}*Ge*	^{75}*As*	^{82}*Se*	^{85}*Rb*	^{88}*Sr*	^{89}*Y*	^{90}*Zr*	^{93}*Nb*	^{98}*Mo*	^{101}*Ru*	^{103}*Rh*	^{108}*Pd*	^{109}*Ag*	^{111}*Cd*	^{115}*In*
A-1	cps	23	2					6						3	4	8102111	15	1
A-2	cps	6			2			3			1				7	8344123	16	
B	cps	25					10	32			5	1			2	8949206	6	2
C	cps	22				2							1	3	18	5753186	1	1
D-1	cps	7		5			1	5							4	9325660	8	
D-2	cps	2				2	4	5								7362250		2
D-3	cps	86		2	54	5		7		5		1		1	2	7111600		
D-4	cps	24	5				4	4		5				3		7409747		
A-1	ppm	0.26												0.006	0.03	39312		0.002
A-2	ppm	0.07			0.02										0.05	40486		
B	ppm	0.28													0.02	43422		0.003
C	ppm	0.82				0.65								0.010	0.23	48200		
D-1	ppm	0.08													0.03	45248		
D-2	ppm	0.02				0.16										35722		0.003
D-3	ppm	2.17			1.8											59600		
D-4	ppm	0.63														62000		

Specimen and laser ablation line	*Unit*	^{120}*Sn*	^{121}*Sb*	^{126}*Te*	^{133}*Cs*	^{138}*Ba*	^{139}*La*	^{140}*Ce*	^{141}*Pr*	^{145}*Nd*	^{151}*Eu*	^{157}*Gd*	^{159}*Tb*	^{162}*Dy*	^{165}*Ho*	^{167}*Er*	^{169}*Tm*	^{172}*Yb*
A-1	cps	23	43		2	3								1				
A-2	cps	31	38	4	4	2				2								
B	cps	26	10		5	16												
C	cps	29	1	8	4	2		3									2	
D-1	cps	85	111		4	1		1										
D-2	cps	56	105	1	3						1					1		
D-3	cps	54	43	2	6	5	3		2									
D-4	cps	28	46		3	3	1											
A-1	ppm	0.10	0.17															
A-2	ppm	0.14	0.15	0.06														
B	ppm	0.11	0.04															
C	ppm	0.21																
D-1	ppm	0.38	0.43															
D-2	ppm	0.25	0.41	0.02														
D-3	ppm	0.39	0.31															
D-4	ppm	0.20	0.33															

Specimen and laser ablation line	*Unit*	^{175}*Lu*	^{178}*Hf*	^{181}*Ta*	^{182}*W*	^{185}*Re*	^{189}*Os*	^{193}*Ir*	^{195}*Pt*	^{202}*Hg*	^{205}*Tl*	^{208}*Pb*	^{209}*Bi*	^{232}*Th*	^{238}*U*
A-1	cps								1	303386			4	1	
A-2	cps							2		285957			6		
B	cps		1			1				281344	16		26		
C	cps									273829			7		
D-1	cps									248113		4	5		
D-2	cps							1	2	197186	2	1	4		
D-3	cps									97195		4	2		
D-4	cps					2				111322		3	2		
A-1	ppm								0.014	1046			0.009		
A-2	ppm									986			0.013		
B	ppm									970			0.055		
C	ppm									1014			0.050		
D-1	ppm									856		0.01	0.010		
D-2	ppm								0.028	680		0.003	0.009		
D-3	ppm									412		0.04	0.02		
D-4	ppm									445		0.03	0.02		

Notes: cps, count per second; ppm, parts per million

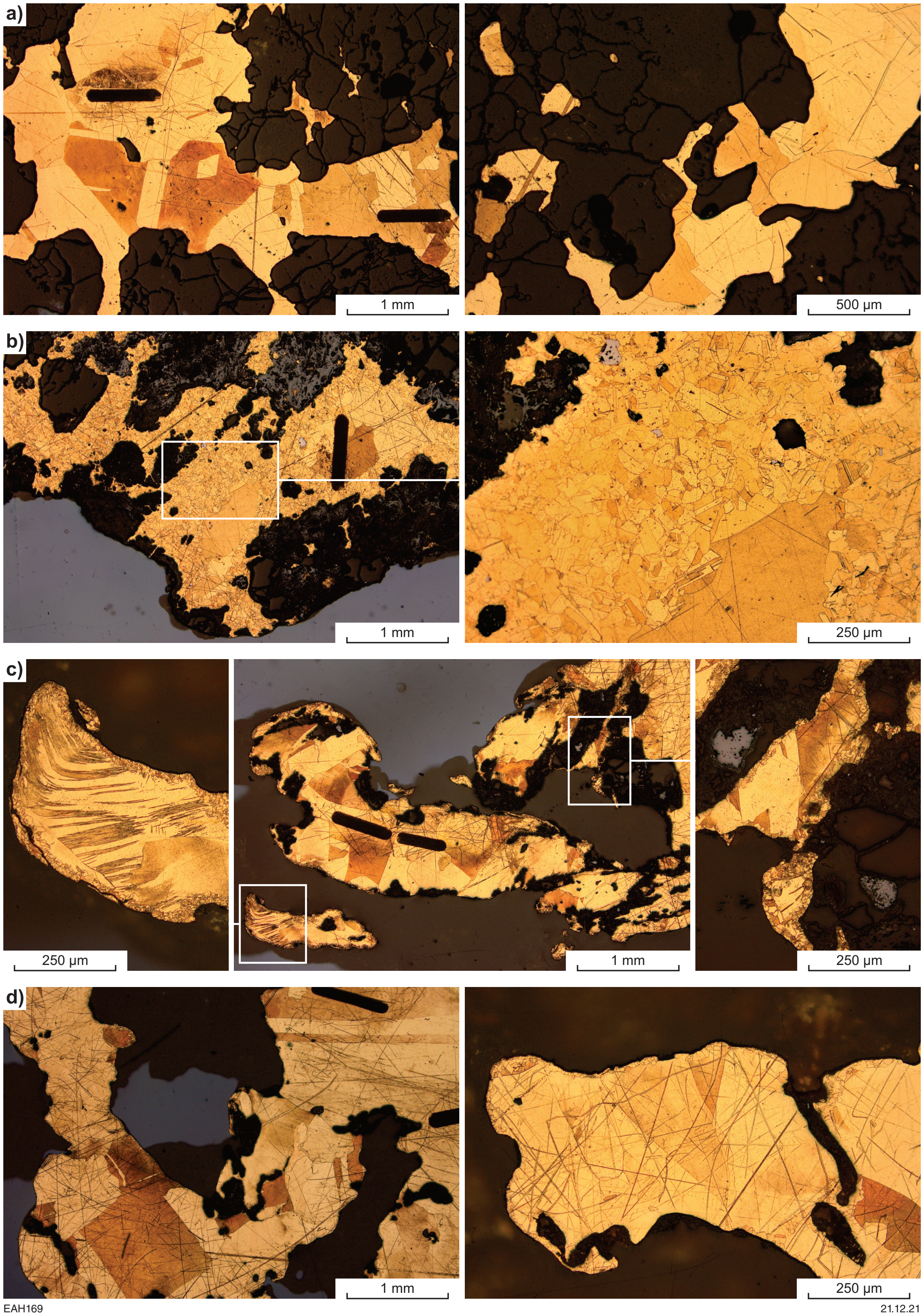

Figure 5. **Reflected-light photomicrographs, after repolishing and acid etching, of parts of sample 201969: gold grains, Coolyia Creek prospect: a) specimen A; b) specimen B; c) specimen C; d) specimen D. Dark elongate lines are laser ablation tracks produced during LA-ICP-MS analyses**

References

Geological Survey of Western Australia 2014, Pilbara, 2014: Geological Survey of Western Australia, Geological Information Series, data package.

Hancock, EA and Beardsmore, TJ 2020, Provenance fingerprinting of gold from the Kurnalpi Goldfield: Geological Survey of Western Australia, Report 212, 21p.

Hickman, AH 2020, Hardey Formation (A-FOh-scb): Geological Survey of Western Australia, WA Geology Online, Explanatory Notes extract, viewed 6 April 2022, <www.dmirs.wa.gov.au/ens>.

Hickman, AH 2021a, East Pilbara Craton: a record of one billion years in the growth of Archean continental crust: Geological Survey of Western Australia, Report 143, 187p.

Hickman, AH 2021b, Kylena Formation (A-FOk-bbor): Geological Survey of Western Australia, WA Geology Online, Explanatory Notes extract, viewed 6 April 2022, <www.dmirs.wa.gov.au/ens>.

Hickman, AH 2021c, Warrawoona Group (A-WA-xb-f): Geological Survey of Western Australia, WA Geology Online, Explanatory Notes extract, viewed 11 May 2022, <www.dmirs.wa.gov.au/ens>.

Hickman, AH and Van Kranendonk, MJ 2008, Marble Bar, WA Sheet 2855: Geological Survey of Western Australia, 1:100 000 Geological Series.

Murray, S 2009, LBMA certified reference materials. Gold project final update: The London Bullion Market Association, Alchemist, no. 55, p. 11–12.

Recommended reference for this publication

Hancock, EA, Blay, OA and Beardsmore, TJ 2022, 201969: gold grains, Coolyia Creek prospect; GSWA Mineralogy Record 3: Geological Survey of Western Australia, 8p.